Emergence of β and γ networks following multisensory training

Daria La Rocca, Philippe Ciuciu, Denis Engemann, Virginie van Wassenhove

Emergence of β and γ networks following multisensory training

Daria La Rocca[a,b], Philippe Ciuciu[a,b], Denis Alexander Engemann[a,b], Virginie van Wassenhove[a,c,*]

[a] *CEA/DRF/Joliot, Université Paris-Saclay, 91191 Gif-sur-Yvette,France.*
[b] *INRIA, Parietal team, Université Paris-Saclay, 91120 Palaiseau, France.*
[c] *Cognitive Neuroimaging Unit, INSERM, Université Paris-Sud, Université Paris-Saclay, NeuroSpin center, 91191 Gif-sur-Yvette, France.*

Abstract

Our perceptual reality relies on inferences about the causal structure of the world given by multiple sensory inputs. In ecological settings, multisensory events that cohere in time and space benefit inferential processes: hearing and seeing a speaker enhances speech comprehension, and the acoustic changes of flapping wings naturally pace the motion of a flock of birds. Here, we asked how a few minutes of (multi)sensory training could shape cortical interactions in a subsequent unisensory perceptual task. For this, we investigated oscillatory activity and functional connectivity as a function of individuals' sensory history during training. Human participants performed a visual motion coherence discrimination task while being recorded with magnetoencephalography. Three groups of participants performed the same task with visual stimuli only, while listening to acoustic textures temporally comodulated with the strength of visual motion coherence, or with auditory noise uncorrelated with visual motion. The functional connectivity patterns before and after training were contrasted to resting-state networks to assess the variability of common task-relevant networks, and the emergence of new functional interactions as a function of sensory history. One major finding is the emergence of a large-scale synchronization in the high γ (gamma: $60-120Hz$) and β (beta:$15-30Hz$) bands for individuals who underwent comodulated multisensory training. The post-training network involved prefrontal, parietal, and visual cortices. Our results suggest that the integration of evidence and decision-making strategies become more efficient following congruent multisensory training through plasticity in network routing and oscillatory regimes.

Keywords: multisensory, motion coherence, acoustic texture, oscillations,

*Corresponding author: e-mail: virginie.van.wassenhove@gmail.com (VvW)

functional connectivity, MEG, audiovisual, learning, confidence, beta, gamma

1. Introduction

The brain can infer the causal structure of its surroundings by integrating multisensory signals originating from the same physical sources, while segregating those originating from different causes [1, 2, 3, 4, 5, 6]. The resolution of this causal inference problem weighs in the reliability and the degree of correspondence between multisensory inputs [7, 8, 9]. In ecological settings, the temporal comodulation of sensory signals helps perceptual scene analysis: for instance, an interlocutor's mouth movements are temporally coherent with the envelope of the acoustic speech signals providing the listener with strong binding cues for predictive inferences [10, 11, 12, 13, 14, 9]. Temporally congruent signals enhance the detectability [15, 9] and the identification [16, 17] of events, whereas temporally incongruent signals hinder their identification [16, 9]. Herein, we explored the cortical mechanisms by which the internalized temporal structure of coherent multisensory events may subsequently regulate visual (unisensory) processing.

Using magnetoencephalography (MEG), we first characterized the impact of uni- and multi-sensory training history on human brain activity when participants ($N = 36$) performed a visual motion coherence task (Figure 1.A). The task consisted in reporting the color of the most coherent cloud of dots amongst two intermixed red and green clouds of moving dots. After initially performing the task with visual stimuli only (PRE), participants were split into three experimental groups for short individualized training during which participants were tested on four strengths of visual coherence centered on each individual's initial discrimination threshold measured in PRE: one group performed the task with visual stimuli only (V), another one with acoustic textures spectro-temporally congruent with the most coherent visual cloud of the two (AV) and a third one, with distracting auditory noise uncorrelated with any of the two visual clouds (CTRL). After performing the training for 20 minutes, all participants were again tested with visual stimuli only (POST). Behaviorally, all participants improved their perceptual discrimination with the AV group showing the largest benefits and with an initial analysis of the MEG evoked activity suggesting the implication of a large-scale brain network following training [17].

With this in mind, we assessed the changes of brain activity between PRE and POST blocks, when all participants performed the unisensory

task with visual stimuli only (Figure 1.B). We thus did not directly focus on the feedforward integration of multisensory features or on selective attention, both of which could only occur during the AV and CTRL training. Here, we thus do not contrast unisensory vs. multisensory processing *per se* but rather focus on the subsequent effects of multisensory integration on a visual only task. Nevertheless, our analytical approach builds on seminal work suggesting the implication of distinct neural oscillatory coupling within large-scale networks [18, 19], [20]). The dynamic regimes mediating the binding of multisensory information across brain regions have started being characterized [21, 18, 19, 22], yet little is known regarding the oscillatory networks which may actively contribute to supramodal or multisensory object representations [14, 17, 23].

Hence, in the present work, we re-analyzed previously collected data and asked how different perceptual histories changed the functional networks hypothesized in [17]. First, initial results suggested that selective attention in this task could not be the primary cause of multisensory benefits considering that the contrasts were ran only when visual stimuli were present. Hence, we did not expect changes in the alpha (α) band network to be the major factor in possible effects of perceptual history in this experimental paradigm. Second, all groups showed behavioral improvement in the task irrespective of their perceptual training; we thus expected changes in the bottom-up (perceptual) analysis of sensory inputs, as captured by high frequency analysis (likely gamma activity, γ). Third, as the AV group improved most, we also expected a strong top-down drive in the POST compared to the PRE for this group. As current research assigns an important role to beta (β) activity in the shaping of top-down predictions and decisional values [24, 25, 26, 27, 28], beta networks were expected to be a major differential driver between the three groups.

To characterize the different oscillatory networks, we estimated oscillatory activity within, and across, experimental groups using univariate time-frequency analyses (Figure 1.C) and large-scale functional connectivity (FC) measures based on the weighted phase lag index (wPLI) [29] (Figure 1.D). We investigated a large network including prefrontal, parietal, occipital and temporal cortices with regions orthogonally selected for their functional relevance in the task (cf [17], see Methods). Among regions of interest were the ventro-lateral prefrontal cortex (vlPFC), a massive site of convergence for visual, auditory and multisensory information processing [30, 31], whose neurons selectively respond to the color of visual objects [32] and low-level abstraction [33]; the intra-parietal sulcus (IPS), which plays a central role in multisensory processing [34, 35, 36] and visual motion area (MT), sensitive

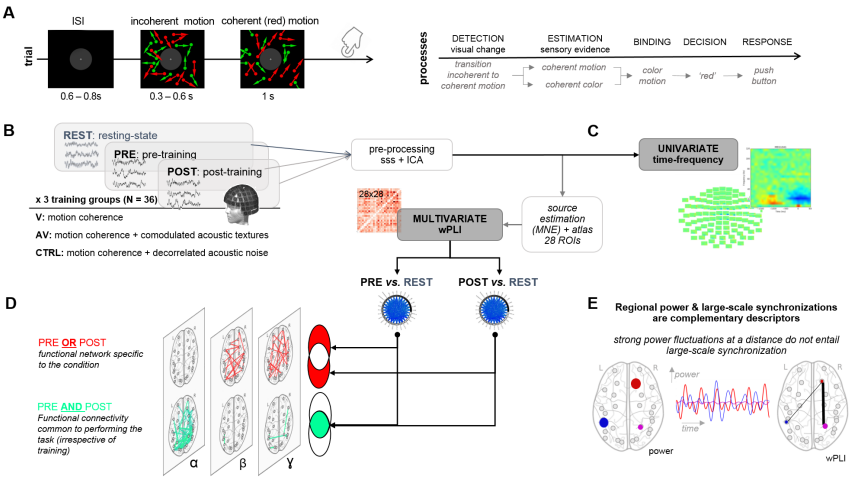

Figure 1: **Experimental procedure and Methods.** (**A**) Left panel: each trial started with the presentation of a fixation cross lasting 0.6 to 0.8 s followed by the presentation of two intermixed clouds of dots moving incoherently. One cloud was red, the other, green. After a variable delay (0.3−0.6 s) of incoherent motion, one of the clouds (here, red) moved coherently for 1 s while the other remained fully incoherent (here, green). Seven possible strength of motion coherence were tested; the direction and color were randomized across trials. Participants selected which of the red or green cloud was most coherent (videos S1 and S2 in [17]). Right panel: schematic operationalization of the motion coherence discrimination task entailing the integration of motion and color for decision-making. (**B**) MEG recordings were collected from 36 participants, who performed the task described in (A) in the PRE and POST blocks. Between the PRE and POST, participants were split in three experimental training groups who performed the task visually (V), with acoustic textures congruent with the most coherent cloud of dot (AV), or with auditory noise uncorrelated with the visual stimuli (CTRL). All new analyses were carried out on the PRE and POST blocks, when all participants were performing the visual task described in (**A**). All participants improved their behavioral scores in POST as compared to PRE blocks: the AV group showed the largest perceptual benefit followed by the V and the CTRL group [17]. Following preprocessing and source estimations, (**C**) univariate time-frequency analysis and (**D**) multivariate functional connectivity analyses were performed to provide (**E**) complementary insights on the oscillatory mechanisms implicated in the effect of (multi)sensory training history in unisensory processing.

to perceptual changes in this task [17]. Both IPS and MT are known to interact in the β range during perceptual decision-making [37]. We first started by exploring the modulation of local oscillatory activity during visual motion discrimination [38, 25], and followed up with the exploration of changes in functional connectivity as a function of sensory history in training.

2. Materials and methods

2.1. Participants

36 healthy human participants were recruited for the study (age range: 18 to 28 y.o.; mean age: 22.1 $\pm$2.2 s.d.; 3 groups of 12 participants each: V: 4 females; AV: 6 females; AVr: 6 females). All participants were right-handed, had normal hearing and normal or corrected-to-normal vision. Before the experiment, all participants provided a written informed consent in accordance with the Declaration of Helsinki (2008) and the local Ethics Committee on Human Research at NeuroSpin (Gif-sur-Yvette, France). Prior to the MEG acquisition, participants were randomly split into 3 experimental groups (V, AV, and CTRL) as detailed below.

2.2. Task

The MEG experiment consisted of interleaved MEG blocks alternating between rest and task. The first resting block occurred prior to any task or training and will be thereafter referred to as REST. REST was used as baseline for functional connectivity analysis. The six task blocks included: a 12 minutes pre-training block (PRE) consisting of the visual coherence discrimination task; a 20 minutes training (4 successive blocks of 5 minutes each) on the same task using purely visual stimuli (V group), congruent audiovisual stimuli (AV group) or incongruent audiovisual stimuli (CTRL group); a 12 minutes post-training block (POST) consisting of the same visual coherence discrimination task as in PRE. Thus, the PRE and POST blocks consisted of the same visual *only* coherence discrimination task for all three experimental groups and using the exact set of visual stimuli. Only the training was either visual or audiovisual. The task requirements in PRE, training, and in POST were otherwise identical in all runs: two clouds of colored dots were intermixed on the screen and participants had to tell which of the red or green cloud of dots was the most coherent. In PRE and POST, participants also rated their confidence on a scale of 1 to 5 after they provided their main response regarding the color of the most coherent cloud of dots.

In PRE and POST, the initial and final motion coherence discrimination threshold of each participant was assessed by testing seven strength of visual motion coherence (15%, 25%, 35%, 45%, 55%, 75% and 95%). 28 trials for each strength of visual motion coherence were collected in PRE and in POST for a total of 196 trials in each block. In the training (4 blocks, 5 min each), four visual coherence levels were tested corresponding to $\pm$ 10% and $\pm$20% of an individuals discrimination threshold computed in PRE (see [17] for more details). 28 trials for each strength of visual motion coherence were presented for a total of 112 trials in a given training block. These data were not considered as our main question focused on contrasting brain activity to identical experimental conditions given a different training history. Further experimental details can be found in [17].

To localize the visual motion area, we used a passive MEG localizer (120 trials) after POST. Participants were presented with a fully incoherent visual cloud lasting 0.5 s and followed by either a highly coherent (95% of coherence) or an incoherent (0% of coherence) interval of 1 s (60 trials each). During the localizer, participants were asked to passively view the visual motion stimuli.

2.3. Stimuli

Visual stimuli consisted of intermixed red and green clouds of dots (Figure 1.A) calibrated to isoluminance using heterochromatic flicker photometry on a per individual basis prior to MEG data acquisition. A white fixation cross was at the center of a 4° gray mask disk and dots were presented within an annulus of 4° to 15° of visual angle. Dots had a radius of 0.2°. The motion flow was 16.7 dots per deg$^2\times$ s with a speed of 10°/s and its direction confined within an angle of $45° - 90°$ around the azimuth. 50% of the trials were upward coherent motion and the remaining 50% of the trials were downward coherent motion. The color and the direction of the most coherent cloud o dots were thus pseudo-randomized across trials and both color and direction were orthogonal to the task goal.

The V group underwent training using visual only stimuli. The AV group underwent training using temporal comodulated audiovisual associations comparable to those used in sensory substitution devices such as the vOICe [39] and the EyeMusic [40], with intuitive perceptual associations between sensory modalities [41, 42]. Here, we used parametric sounds or acoustic textures (cf [43] with sampling frequency = 44.1 kHz, frequency range: 0.2 to 5 kHz) which enabled to pair each visual dot with a linear frequency-modulated acoustic sweep whose slope depended on the direction taken by

the visual dot (see [17] for more details). The maximal slope was 16 octaves/s corresponding to motion directions of $82.9° - 90°$. A visual dot moving upwards was associated with an upward acoustic ramp, whereas a downward moving dot was associated with a descending acoustic ramp. The duration of a ramp was also identical to the life-time of a visual dot. The CTRL group underwent training with acoustic noise of the same duration and amplitude as the acoustic textures used for the AV group. Unlike acoustic textures in which the dynamical properties of the fine spectral acoustics were matched with the dynamical properties of the visual dot motion, the acoustic noise used for the CTRL group was fully uncorrelated with the visual coherent motion. This served as a control so that participants trained with audiovisual signals could either hear a sound designed to be temporally predictive of visual coherence (under the temporal comodulation hypothesis, automatic mapping between the spectral coherence in acoustics and visual motion coherence; AV group) or a random acoustic noise (the lack of spectral coherence in the acoustics could not map on visual motion coherence and may act as a distractor). In sum, the CTRL group was included to test the specificity of audiovisual associations in this task and the benefit of temporal comodulation in audiovisual training.

In the task and for all experimental groups, a given trial started with a variable duration (0.3 to $0.6s$) mixing both red and green clouds of dots being fully incoherent (0% of coherent motion). Then, one cloud of dots became more coherent than the other for a duration of one second. In PRE and POST, the coherence level taken by the most coherent cloud was one of seven possible values described in the Task section. During training, the coherence level taken by the most coherent cloud took one of four values described in the Task section. Inter-trials intervals (ITI) varied from 0.6 to $0.8s$. Samples of the video trials can be experienced (Movies S1 and S2 in [17]).

2.4. MEG and MRI data acquisition

Electromagnetic brain activity was recorded in a magnetically shielded room using a 306 MEG system (Neuromag Elekta LTD, Helsinki). MEG signals were sampled at 2 kHz and band-pass filtered between 0.03-600 Hz. Four head position coils (HPI) were used to measure the head position of participants before each block; three fiducial markers (nasion and pre-auricular points) were used during digitization as a reference for coregistration of anatomical MRI (aMRI) immediately following MEG acquisition. Electrooculograms (EOG) and electrocardiogram (ECG) were recorded simultaneously with MEG. Five minutes of empty room recordings were acquired

before each block for the computation of the noise covariance matrix. The T1 weighted aMRI was recorded using a 3-T Siemens Trio MRI scanner. Parameters of the sequence were: field-of-view: $256 \times 256 \times 176$ mm^3 (transversal orientation), voxel size: $1.0 \times 1.0 \times 1.1$ mm; acquisition time: 466 s; echo time TE = 2.98 ms, inversion time TI = 900 ms, repetition time TR = 2300 ms and flip angle (FA): 9°. For each participant, cortical reconstruction and volumetric segmentation of T1 weighted aMRI was performed using FreeSurfer[1]. Once cortical models were complete, deformable procedures were executed using the MNE software [44] to register source estimates of each individual onto the FreeSurfer average brain for group analysis.

2.5. MEG preprocessing

The analysis of the MEG data was carried out using the MNE-python toolbox [45]. After applying an anti-aliasing FIR filter (low-pass cutoff frequency at 130 Hz), MEG data were down-sampled to 400 Hz, and preprocessed (Figure 1.B) to remove external and internal interferences, in accordance with accepted guidelines for MEG research [46]. Signal Space Separation (SSS) was applied with MaxFilter to remove exogenous artifacts and noisy sensors [47]. Ocular and cardiac artifacts (eye blinks and heart beats) were removed using Independent Component Analysis (ICA) on raw signals. ICA were fitted to raw MEG signals, and sources matching the ECG and EOG were automatically found and removed before signals reconstruction following the procedure described in [44][2]. On average, and over the 36 participants: 39.149.91 components were extracted and 3.250.86 components were zeroed out for the REST conditions; 418.79 components were extracted and 4.301.39 components were zeroed out for TASK.

2.6. Univariate time-frequency analysis in sensor space

Briefly, to identify significant changes in oscillatory activity associated with task performance and task improvements, we performed non-parametric cluster-level 1 sample t-tests for each frequency band. Second, in PRE, we performed non-parametric cluster-level paired t-test on time-frequency epochs (single-trial analysis), contrasting high and low motion coherence as well as correct and incorrect trials. Third, we performed non-parametric

[1] http://surfer.nmr.mgh.harvard.edu/

[2] https://github.com/mne-tools/mne-python/blob/master/tutorials/plot_artifacts_correction_ica.py

cluster-level paired t-tests on time-frequency epochs, contrasting brain activity to the same stimuli in PRE and POST blocks. The details of each statistical test is provided below.

The oscillatory activity in α, β and γ ranges was established using a univariate time-frequency analytical approach in sensor space(Figure 1.C). Oscillatory activity in the post-stimulus period was contrasted with the pre-stimulus period. Both the duration of the initial incoherent portion of stimuli (300 to 600 ms) (Figure 1.A) and the decision time reflected in reaction times (RTs) were variable. As such, we locked the epochs according to three different events in the sequence of stimuli, each relevant for our ad-hoc working hypotheses and inherent to our experimental design. A first epoching ranged from -600 ms to $+900$ ms *post-incoherent* motion onset thus fully capturing the incoherent portion of the stimuli. The second epoching focused on the brain activity following the onset of motion coherence *per se* and ranged from 0 ms to $+1500$ ms *post-coherent* motion onset. The third epoching focused on the decision-making analysis and was anchored on RTs from -1000 to $+500$ ms around the *button press* (RT). For all three sets of epochs, the 600 ms interval preceding the incoherence onset served as baseline activity.

For each set of epochs, a group-level non-parametric spatio-temporal cluster analysis was computed on single-trial time-frequency transforms obtained with Morlet complex-valued wavelets and averaged in each frequency band of interest. The number of cycles in the Morlet wavelet was defined for each frequency (f) as $f/2$. To assess the statistical significance of the obtained clusters we randomly flipped $r = 10^4$ times the sign of the time-frequency transformed data, and our cluster-level correction for multiple comparisons was based on the maximum statistic method [48]. The spatio-temporal clustering was used to identify the sensors showing significant event-related activity in PRE and in POST. One of these sensors was used for subsequent univariate analyses to ensure that any inference made on a particular frequency band was first determined independently of our ad-hoc working hypothesis motivating the subsequent contrasts. Specifically, time-frequency cluster analyses were used in PRE to perform group-level statistics ($N = 36$, low *vs.* high MC, and correct *vs.* incorrect trials). Moreover, a statistical contrast was performed between POST and PRE blocks, pooling all participants together ($N = 36$) as well as considering each group separately ($N = 12$). Statistical significance for all these contrasts was assessed using random permutations as discussed above.

To evaluate the extent to which oscillatory activity could significantly contribute to the observed behavioral measures (performance, RTs, confidence)

and stimulus parameters (strength in visual motion coherence), we used a post-hoc general linear model (GLM) on single trials over the time intervals found to be significant in our cluster analyses. The non-parametric approach to GLM based on random permutations was employed to obtain a robust and unbiased linear regression [49, 50]. The GLM to test the linear regression between oscillatory power and the strength of visual motion coherence and different behavioral parameters followed the equation $y = \mathbf{w^T x} + \epsilon$. Here, $y \in \mathbb{R}$ was the MEG mean power in a significant cluster of sensors; $\mathbf{x}$ was the vector $[1, x_1, x_2, \cdots, x_{p-1}]^T \in \mathbb{R}^p$ containing p regressor variables. To find the best fitting model, we tested different combinations of regressors including motion coherence, reaction times, correctness, confidence ratings and their interactions. Each regressor was first tested in an independent linear model, and significant explanatory variables were subsequently tested in the same model, together with their interactions in order to identify possible driving effects.

$\mathbf{w}$ contained the p regression coefficients including the constant term, and ϵ was the error term. Iteratively reweighted least squares were used to obtain an estimate of $\mathbf{w}$ and a value of the Wald statistic w_{ref}. A non-parametric approach based on random permutations was used to obtain robust and unbiased significance levels and confidence intervals. Specifically, to test the significance of each estimated regression coefficient w_i, $r = 10,000$ random permutations of the corresponding regressor variable x_i were generated, yielding a distribution of Wald statistics w^* for each partial regression coefficient under the null hypothesis $H_0 : w_i = 0$. For each estimated coefficient, the p-value was calculated as the proportion of w^* grater then or equal to w_{ref}, in absolute value. Permutation inference for the GLM in common neuroimaging applications has been proposed as a non-parametric test to relax assumptions on data distributions [51]. The 36 participants were pooled together in PRE ($N = 36$) whereas group-specific analyses ($n = 12$) were performed on POST data to study the effects of (multi)sensory training. This analysis was carried out for the three sets of epochs locked to the three different events (incoherence onset, coherence onset, response).

2.7. MRI-MEG coregistration and source reconstruction

The coregistration of MEG data with the individual anatomical MRIs (aMRI) was carried out by realigning the digitized fiducial points with the markers in MRI slices, using MRILAB (Neuromag-Elekta LTD, Helsinki) and *mne_analyze* tools within MNE ([44]). Individual forward solutions for all source reconstructions located on the cortical sheet were computed using a 3-layers boundary element model constrained by the individual aMRI.

Cortical surfaces were extracted with FreeSurfer and decimated to about 5,120 vertices per hemisphere with 4.9 mm spacing. The forward solution, noise and source covariance matrices were used to calculate the noise-normalized dynamic statistical parametric mapping (dSPM) ([52]) inverse operator (depth = 0.8). The inverse solution was obtained using a loose orientation constraint on the transverse component of the source covariance matrix (loose = 0.4). The estimates of the reconstructed dSPM time series were interpolated onto the FreeSurfer average brain for group-level source space analysis. Only the radial components of the estimated currents were considered for further analysis.

After source estimation, we proceeded by summarizing the results into regions of interest (ROIs). When selecting the ROIs, we encountered the well-known trade-off between computational tractability and signal-to-noise ratio: Too small ROIs (e.g., voxel-wise analysis) may increase the noise and at the same time exacerbate the multiple comparisons problem, while too large ROIs may suffer from signal cancellation, especially if multiple sources are captured in one ROI. In MEG and EEG source localization, additional peculiarities have to be considered. First, source reconstructed spatial maps are coarser and more blurred than in fMRI, hence potentially arguing in favor of using coarser parcellations. Second, the sign of the reconstructed signals follows the curvature of the cortex which may induce cancellation during averaging. This may distort resulting time-courses even if only one single source is captured by the ROI. In practice, ROIs are therefore often selected according to specific data analysis goals [53, 54, 55] as is generally recommended for many elements of MEG and EEG analysis [56]. In light of these considerations, we chose the rather coarse Desikan-Killiany parcellation [57] from FreeSurfer that covers both hemispheres on each individual cortex with 28 ROIs [3]. This set of ROIs has already been established as sufficiently sensitive in previous work from our group. For example, it has been shown to capture multisensory processing, perceptual decision making and motion discrimination [17]. To mitigate the risk of potential signal cancellation, we used a weighted averaging approach, which explicitly took into account the cortical curvature through the surface normals. The resulting ROIs covered the frontopolar regions (FP), frontal eye field (FEF), ventro-lateral prefrontal cortex (vlPFC), premotor cortex and supplementary motor region (BA6), primary motor cortex (PMC), intra-parietal sulcus (IPS), inferior temporal cortex (ITC), auditory cortex (AUD), superior tem-

[3] https://surfer.nmr.mgh.harvard.edu/fswiki/CorticalParcellation

poral sulcus (aSTS, mSTS and pSTS), middle temporal visual area (MT), visual area V4, and primary and secondary visual cortices (V1-V2). The average activities over all the vertices within each of these cortical regions (labels) were used for the subsequent functional connectivity analysis.

2.8. Functional connectivity analysis

2.8.1. Adjacency matrices

Functional interaction between brain regions was assessed by evaluating the similarity of brain activity across remote brain areas, namely functional connectivity (FC) (Figure 1.D). Several studies have compared a subset of FC methods with respect to their ability to correctly detect the presence of simulated connectivity schemes in a multivariate data set [58]. The outcomes showed that the performance of the measures depended both on the characteristics of the dataset and the methods. No single method outperformed the others in all cases. A practical and reasonable approach thus consisted in predetermining the FC method according to the plausible ad-hoc working hypotheses of the experimental study under scrutiny. To characterize FC in the absence of *a priori* knowledge about its nature and the generating model, non-parametric measures could first be used.

The notion of phase coupling derives from the study of oscillatory nonlinear dynamical systems. Based on this notion, Phase Lag Index (PLI) [59] aims at quantifying in a statistical sense the phase delay between such systems from experimental data [60] according to the following formula:

$$PLI_{ij} = |\mathbb{E}\{\text{sign}[\Delta\Phi_{ij}(t_k)]\}|, \in [0, 1] \tag{1}$$

where $\Delta_{ij}\Phi(t_k) = \Phi_i(t_k) - \Phi_j(t_k)$ quantifies the instantaneous phase difference between two source reconstructed time series $s_i(t)$ and $s_j(t)$ at time point $t = t_k$. In Eq. (1), the expectation is typically replaced by the empirical mean over consecutive time points. PLI was shown to be robust with respect to instantaneous linear mixing effects which may lead to the detection of spurious functional couplings not caused by brain interactions (instantaneous linear mixing effects) [59].

Moreover, PLI has the advantage of not being influenced by the magnitude of phase delays. Weighted PLI (wPLI) also solves the problem of discontinuity around zero [29], by using the magnitude of the imaginary part of the cross-spectrum as weights. To measure pairwise interactions between the extracted cortical labels, we used the definition of wPLI in the frequency domain, exploiting the phase of the Fourier-based cross-spectrum $S_{i,j}(f)$ of

two time series $s_i(t)$ and $s_j(t)$:

$$wPLI_{ij}(f) = \frac{|\mathbb{E}\{|\Im\{S_{ij}(f)\}|\text{sign}(\Im\{S_{ij}(f)\})\}|}{\mathbb{E}\{|\Im\{S_{ij}(f)\}|\}}, \in [0, 1] \quad (2)$$

where $\Im$ stands for the imaginary part, and the expectations were replaced by their empirical estimates averaged over epochs. Here, f usually spans a specific frequency band such as oscillatory regimes (α, β or γ). Therefore, each FC observation consisted of a symmetric adjacency matrix of size 28×28. 10 instances of FC were obtained for each participant and each block performing a partition of epochs into 10 non-overlapping subsets. In order to ensure the balance of the number of epochs used to obtain each FC instance for the different participants, the total number of epochs was set to the minimum observed across participants.

2.8.2. Statistical analysis of FC

A widely employed approach to extract the FC network of interest from an adjacency matrix consists in applying a threshold to the strength of the estimated connections (Figure 4.A). The threshold is obtained according to a suitable criterion [61]. The resulting FC patterns correspond to the strongest connections, which do not necessarily reflect the most significant differences between experimental conditions. Additionally, while such approach is particularly suitable for graph-theoretic network analysis, it does not allow direct quantitative comparisons, owing to the variability of significant connections.

Here, our goal was to separately investigate the FC changes that were task-dependent (*i.e.* significant changes in the contrast PRE or POST *vs.* REST) and the cortical interactions subsequent to (multi)sensory training in each group. Hence, the comparison between FC estimates obtained for the three experimental groups (V, AV, CTRL) was addressed using a different approach. First, adjacency matrices were separately averaged over each frequency band of interest, each block (REST, PRE and POST) and each participant (Figure 4.A). Second, for each frequency band and each experimental group (V, AV and CTRL), the task-relevant networks were extracted by performing a group-level permutation t-test between FC estimated in REST and FC estimated in task blocks (PRE, POST) (Figure 4.B). Third, considering only the subset of task-related connections common to PRE and POST blocks (i.e. the connections significantly changing both in PRE and POST as compared to REST), the variability driven by the perceptual history training (POST *vs.* PRE) was evaluated using a permutation t-test (Figure 4.C, top).

All statistical tests were corrected for multiple comparisons using the maximum statistic method [48]. Finally, the reorganization of FC in POST was addressed by highlighting the emergence of new task-relevant FC in POST, which were not observed in PRE (Figure 4.C, bottom). Importantly, this approach considered the FC at REST as the baseline for all other FC analyses. This allowed to better disentangle the different FC patterns and their changes between PRE and POST. Hence, a linear correlation analysis based on Pearson's correlation coefficient was performed between the average increase of post-specific interactions from PRE to POST, and the corresponding increase of confidence ratings, for each frequency band and each training group separately.

2.8.3. Topological analysis of FC

A complementary and conventional topological analysis of FC networks was also carried out [62] to investigate the degree of interaction between each brain region per oscillatory regime. Specifically, the networks with density threshold given by $3/N_{rois}$, where N_{rois} is the number of regions [63], were first extracted for each participant, each block and each frequency band. The weighted node degree D_i, a topological property which is a conceptually simple measure of centrality of a node i within a network, was then computed for each label in the extracted networks, according to the formula:

$$D_i = \sum_{k=1}^{K} r_{i,k} \tag{3}$$

where K is the number of nodes in the network (cortical labels), and $r_{i,k}$ is the estimated FC value between nodes i and k. Permutation t-test were performed to evaluate the differences of node degree values between REST and task blocks (i.e. PRE or POST) as well as between PRE and POST. Again, the maximum statistic method was used to correct the statistical tests for multiple comparisons [48].

3. Results

We first assessed the broad-band oscillatory activity following the presentation of visual motion stimuli. For this, we combined single-trials in PRE, which were evoked by all motion coherence levels in all three experimental groups ($N = 36$), and performed a time-frequency analysis of the MEG responses. A spatio-temporal clustering permutation test corrected for multiple comparisons (see Experimental Procedures) on post-stimulus

time-frequency activity (Figure 2.A, left panel) revealed a significant decrease of α (alpha: $7-14Hz$) and β ($15-30Hz$) power ($p < 0.001$, starting 0.09 s post-incoherence onset to 0.31 s post-response; 38 sensors) with a significant increase in the power of broadband high γ ($60-120Hz$, $p < 0.001$, starting 0.04 s post-incoherence onset to 0.62 s post-response; 24 sensors) as compared to baseline. The significant clusters observed for both the sustained decrease in α power and the increase in high-frequency γ power were mostly localized in the occipital sensors (Figure 2.A, middle panel). This pattern lasted throughout the presentation of visual motion coherence. Consistent with the topographical pattern at the scalp level, source estimations of the α and the high γ responses suggested generators located in bilateral visual cortices (Figure 2.A, right panel). This time-frequency pattern during unisensory visual motion coherence was consistent with previously reported time-frequency responses induced by visual motion stimuli [64, 38]. The significant increase in γ band during visual motion coherence was also consistent with a previous report of visual motion eliciting a stronger γ response than stationary visual stimuli [65]. We then asked whether the post-stimulus power changes in α, γ, and β were linked to the strength of visual motion coherence in PRE (for all participants) and in POST (as a function of the experimental group), and then proceeded with the exploration of the β band.

3.1. α suppression is independent of sensory evidence and training history

In PRE, *i.e.*, prior to any training, we used the grand average data ($N = 36$) and assessed changes in α power from the onset of motion coherence (Figure 2.A, left panel, white demarcation lines) as a function of the strength in motion coherence (Figure 2.B) using non-parametric statistics and a GLM. We found no significant relationships between α power and motion coherence. The same regression analysis was performed in the POST data, independently for each experimental group ($N = 12$) in order to preserve the distinct training history of each group. Again, we found no significant relationships between α power and motion coherence, and no significant differences in α power between PRE and POST experimental blocks. Overall, we found no substantial evidence that α power varied as a function of visual motion coherence strength or perceptual history. While the absence of systematic α modulation limits the functional specificity of α in this task, the general decrease of α power notably seen in posterior sensors during the presentation of visual stimuli was generally consistent with the inhibitory gating of visual information [66, 67] thereby a decrease in α power could be taken as an index of selective attention [68].

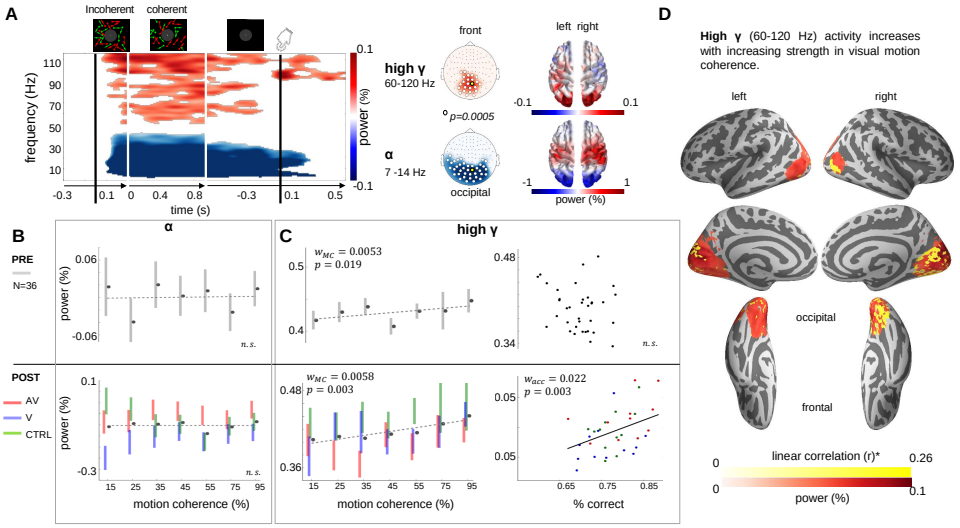

Figure 2: **Occipital low-frequency suppression and motion strength (and POST-accuracy) dependent broadband γ increase**. (**A**) Significant occipital time-frequency clusters of low-frequency (< 45 Hz) power suppression and γ ($45 - 120$ Hz) band increase were found during the presentation of motion coherence (left panel). The time-frequency analysis was locked to the onset of incoherent motion (first black vertical line) and to the coherence motion onset (first white vertical line; the second white vertical is the offset) as well as response-locked (second black vertical line). The three separate analyses were stacked together to provide the full unfolding of oscillatory activity during the trial. The group average ($N = 36$) time-frequency response of the PRE trials showed a sustained decrease of low-frequency power with an increase in broadband γ power: this is illustrated for one occipital sensor in the obtained spatial clusters (highlighted yellow sensor in the central panel; see also Inline Supp. Mat.A). Source estimates of α ($7 - 14$ Hz) power and broadband γ revealed the implication of visual and parietal cortices (right panel). (**B**) In occipital sensors, we found no significant modulations of α power as a function of motion coherence in PRE (top panel) or in POST (bottom panel). Bars are 1 s.e.m. (**C**) High γ activity increased with motion coherence in PRE (left top panel) and in POST (left bottom). High γ activity also increased with accuracy but only in POST (right bottom). Bars are 1 s.e.m. (**D**) Source estimates showed a significant linear relationship between high γ and motion coherence in occipital cortices.

3.2. Broadband high-γ power increases with the strength in visual motion coherence and post-training performance

Before training (PRE, $N = 36$), the occipital broadband high γ following the presentation of visual motion coherence showed a significant increase with the strength of visual motion coherence ($w_{MC} = 0.0053, p < 0.05$; Figure 2.C, left top panel). A similar analysis performed on POST data separately for each experimental group ($N = 12$) revealed a significant linear relationship between the post-stimulus γ power increase and the increase in stimulus motion coherence. This effect was seen in all three groups irrespective of training history ($w_{MC} = 0.0058$, $p < 0.05$; Figure 2.C, left bottom panel). This observation was consistent with the important role of high γ power during motion discrimination and its modulation by the strength in visual motion ([38]. In PRE, no other effects or interactions were found when adding participants' behavioral correctness (C), reaction times (RT), or confidence ratings (CR) to the GLM (see Experimental Procedures; additional information regarding behavioral outcomes provided in (Figure **??** and [17]). To the contrary, in POST, a positive interaction between correctness and motion coherence drove the regression analysis on its own ($N = 36$, $w_{MC-C} = 0.0055$, $p < 0.005$). In fact, irrespective of training history, the interaction between the strength of motion coherence and participants' performance explained the linear relationship between participants' correctness and occipital broadband high γ power ($w_{C_{tot}} = w_{C:MC} = 0.0055 \times MC$, $p < 0.005$; see Figure 2.C, right panels). Subsequent source estimations (see Experimental Procedures) suggested that the increased modulation of high γ band activity likely originated in visual cortices (Figure 2.D). This observation was in general agreement with previous findings linking local γ band activity to the encoding of sensory evidence [69] during a visual motion discrimination task [38, 25], and suggested that irrespective of sensory history in training, the reliability of visual sensory evidence contributed to successful task performance.

In addition to the post-stimulus α and γ effects found in PRE ($N = 36$), we also observed two significant β clusters ($15-30Hz$) partially overlapping over the frontal sensors during the presentation of coherent motion: a bilateral early increase in β band power ($p < 0.005$, from 0.26 s pres-coherence onset to 0.65 s post-coherence onset, 40 sensors) was subsequently followed by a significant decrease ($p < 0.005$, 21 sensors) over the left hemispheric sensors. The decrease in β band power started around 0.57 s following the onset of visual motion coherence (Figure 3.A). The same analysis performed on POST data ($N = 36$) showed, overall, that the decrease in β power was left-lateralized and occurred more strongly over left frontal sensors. In what

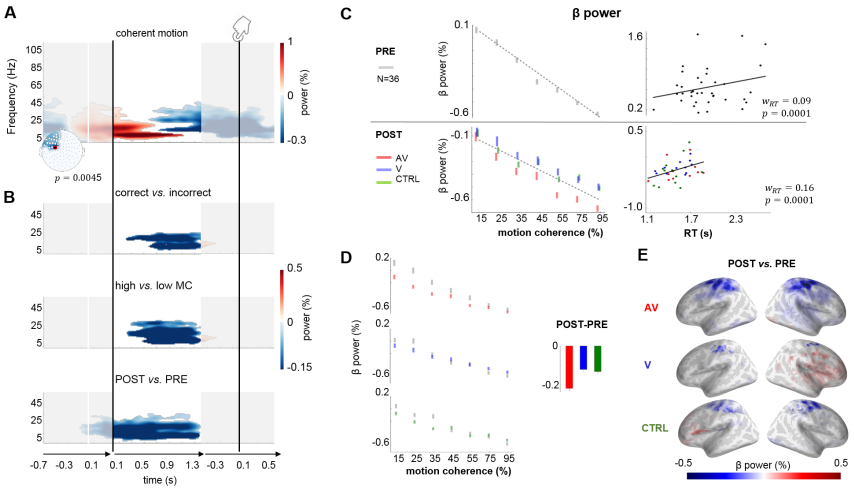

Figure 3: **The modulations of β power activity indicate a gain in efficiency**. (**A**) Group average ($N = 36$) time-frequency maps during the PRE block. The analysis was separately performed on trials locked to the incoherent stimulus onset (white vertical line), locked to the coherent motion (first black vertical line) and locked to the response (second black vertical line). All three analyses were stacked for illustration and provided for a left hemispheric sensor (red dot on left topographic map). Time-frequency permutation clustering statistics revealed two β ($15 - 30$ Hz) components partially overlapping over frontal sensors (topography and represented sensor reported on the bottom right corner) during the presentation of the coherent dot motion: a significant bilateral early increase of β power (red) was followed by a significant decrease solely over the left hemispheric sensors. (**B**) Statistical contrasts tested the changes in β power between correct *vs.* incorrect trials (top panel), high *vs.* low motion coherence trials (middle panel) and POST *vs.* PRE trials (lower panel). All three contrasts revealed a stronger decrease of β power. See also Inline Supp. Mat.B (**C**) Consistent with contrasts in (B), β power linearly decreased with increasing motion coherence in PRE and in POST (left top and bottom, respectively) but linearly increased with RT in PRE and POST (right top and bottom, respectively). (**D**) The AV group showed the strongest β power decrease from PRE (gray) to POST (red) for all strengths of visual motion coherence (left panel). Bars are 1 s.e.m. Thus, during motion coherence stimuli the strongest overall β power decrease from PRE to POST was observed for the AV group (histogram on the right). Source estimates of β power showed a significant decrease in POST as compared to PRE over (E) the motor and parietal cortices. This effect was strongest for the AV group.

follows, we thus further investigate changes in β power.

3.3. Distinct β power effects

In a first working hypothesis, we considered prior work showing that changes in β power contribute to perceptual decision-making [37, 70], also that motor β power can be modulated by attention when anticipating motion coherence onset [71] and may index functional inhibition during perceptual discrimination tasks engaging different sensory modalities [72, 73]. To test whether these affected the observed the significant β power suppression in our study, we performed cluster permutations on time-frequency data locked to the onset of motion coherence, and devised three contrasts of interest (Figure 3.B): correct *vs.* incorrect trials in PRE as in [37] (top panel), high *vs.* low motion coherence in PRE (middle panel) and PRE *vs.* POST trials (bottom panel). In all three contrasts, we found a significant decrease of β power so that the *a priori* easiest trials yielded a larger suppression of β power compared to the more difficult trials. Specifically, we found a systematic late decrease of β power in the correct *vs.* incorrect trials ($p < 0.05$, starting 0.28 s post-coherence onset; Figure 3.B, top) and in the high *vs.* low motion coherence contrast ($p < 0.01$, starting 0.22 s post-coherence onset; Figure 3.B, middle). A similar, yet longer-lasting, left-lateralized frontal β effect was found in the POST *vs.* PRE contrasts ($p < 0.01$, 0.08 s pre-stimulus onset; Figure 3.B, bottom).

As the decrease in β power was found locked to the coherence onset but late in the trial – i.e. just before participants' responses –, it may have reflected the seminal β suppression preceding movement onset [74] seen when locking epochs to the individuals' reaction times (RT) (Figure 3.A, second black line). To test for the possibility that the observed β suppression reflected β event-related desynchronization shaped by motor readiness and action execution [75, 76], we thus locked the trials to participants' RT and tested the same contrasts as those performed previously on the trials locked to the onset of motion coherence (*i.e.*, correct *vs.* incorrect in PRE data, high *vs.* low motion coherence in PRE data and PRE *vs.* POST). The correct *vs.* incorrect, and the high *vs.* low motion coherence response-locked contrasts did not reveal a decrease but, instead, a small but significant increase ($p < 0.05$ starting around 0.6 s before movement onset) of β power before movement preparation. This pattern was only detected when locking the data to the RT (Figure 3.B first two rows on the right) and was distributed over the posterior and frontal sensors. This effect appeared to converge with previous observations [25], in which β power was suggested to

mediate stages of decision-making linking sensory evidence encoding with choice-related action execution. We did not observe significant differences when contrasting the PRE and POST activity for this effect (Figure 3.B third row on the right), and thus did not pursue the analysis of this specific effect which had been previously investigated in details [25]. Importantly however, this response-locked β activity did not seem to be shaped by sensory history in training, and the changes in β power locked to the onset of visual motion coherence (Figure 3.A and Figure 3.B) were thus considered distinct from the seminal response-locked effect.

3.4. β power is sensitive to integrated evidence during decision-making

Considering that the modulations of β power suppression were not specific to the presentation of visual motion coherence, but rather also sensitive to the correctness and the type of training participants underwent, we tested whether, in the absence of a task, the same β power decrease could be seen. For this, we used the localizer data during which participants passively attended the coherent motion stimuli in the absence of a task. We contrasted brain responses elicited by the presentation of coherent motion with those obtained in response to the incoherent motion. We found no significant β power changes in this contrast, suggesting that being engaged in the discrimination task was necessary to observe the β suppression effects.

We then performed a separate regression analysis (GLM) on the PRE ($N = 36$) and the POST data (independently for each experimental group, $N = 12$) (Figure 3.C, top and bottom panels, respectively). We used the strength of motion coherence and three behavioral variables (correctness, RT, confidence ratings) as regressors. With this approach, we assessed which of the stimulus motion coherence or of the three behavioral outcomes, contributed most to the variance of the observed modulation in β power. We found that β power significantly decreased with increasing strength in motion coherence in PRE ($N = 36$, $w = -0.08$, $p < 0.001$), (Figure 3.C, left top panel). We also found a significant positive interaction between motion coherence and RT ($N = 36$, $w = 0.02$, $p < 0.001$; (Figure 3.C, right top panel)): in other words, for a given strength of visual motion coherence, we observed a decrease of β power with faster RT. Altogether, we thus observed that the strongest visual motion coherence and the fastest RT showed the lowest β power.

We then applied the same regression analysis on POST data separately for the three experimental groups ($N = 12$). To make the group-specific results comparable, β power from PRE data were separately subtracted from each individual group's POST data. This analysis revealed a decrease in

the slope of the regression between β power and the strength of visual motion coherence in all three experimental groups (Figure 3.C, bottom left). This was consistent with the fact that all participants improved their performance after training with increased accuracy, decreased RT, and increased confidence rating [17]. Similar to the PRE effects, we found a positive interaction between the strength of visual motion coherence and RT with β power (Figure 3.C, bottom right). Crucially, an overall decrease of β power from PRE to POST was consistently observed for all levels of visual motion coherence in the AV group as compared to the V and the CTRL groups (Figure 3.D). That motion coherence and RT were the main contributors to the β power variability was consistent with the observation that all experimental groups were faster in POST as compared to PRE. Interestingly however, that the AV group displayed the largest decrease of β power overall after training was also consistent with its overall better performance compared to the other groups (and not with a faster response as the RT were comparable across groups, [17]). In other words, each group showed an overall decrease of β power as a function of the strength of visual motion coherence, which may indicate an overall gain in stimulus processing efficiency as the regression slopes across groups were comparable (Figure 3.D, left panel). Additionally, this decrease was shifted down for the AV group as indicated by the histogram in Figure 3.D, which shows the overall difference (mean and s.e.m. over subjects) of β power between POST and PRE for each group, separately. Finally, the performance on the task showed a significant correlation with β power but only when using an independent linear regression model, suggesting that motion coherence and RT contributed most to the β power effects, which in turn affected performance.

To sum up our observations on β power locked to the onset of visual motion coherence: the task-related decrease in β power over the frontal sensors got generally stronger with integrated evidence to perform the task. Additionally, congruent multisensory training (AV) induced a larger (POST-PRE) decrease of β power than other unisensory (V) or conflicting audiovisual (CTRL) trainings. Consistent with the sensor data, the POST *vs.* PRE statistical contrasts of source estimates showed a strong β power decrease over parieto-central regions especially for the AV group; this decrease was also observed in the V and in the CTRL groups to a smaller extent (Figure 3.E). The observed β power suppression during motion coherence discrimination converges with previous literature reporting a central role of β power during perceptual decision making tasks [77, 37, 70].

As interim summary for the univariate oscillatory analysis, we observed that α and broadband γ responses during the presentation of visual coher-

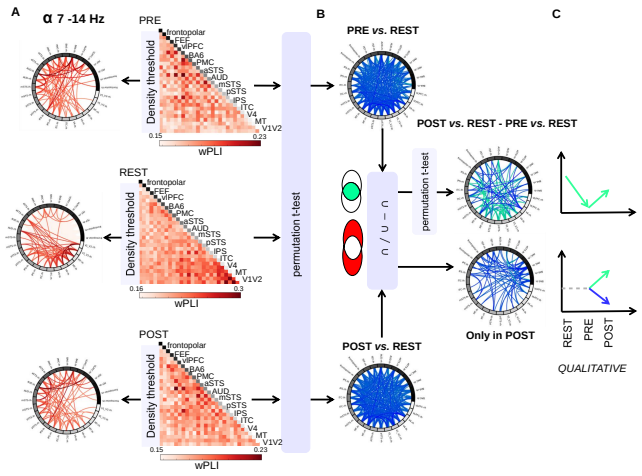

Figure 4: **Overview of statistical contrasts performed to extract functional oscillatory networks.** (**A**) Functional connectivity (FC) estimates during the presentation of coherent motion, in PRE and in POST, contrasted with resting-state FC patterns (REST). For illustration, we report the full and thresholded α oscillatory networks separately for PRE, REST and POST (top to bottom panels, respectively). Statistical contrasts were based on non-parametric permutation t-tests and performed on the 28 cortical regions. (**B**) Pairwise phase couplings were contrasted to show significant differences of weighted Phase Lag Index (wPLI) values characterizing the task-related FC network (PRE *vs.* REST and POST *vs.* REST). (**C**) The FC patterns computed in (B) were compared to assess the variability of the task-related FC in PRE and in POST, as well as to characterize the appearance of new connectivity patterns in POST. FP: frontopolar; FEF: frontal eye field; vLPFC: ventro-lateral prefrontal cortex; PMC: primary motor cortex; BA6: supplementary motor cortex; IPS: intra-parietal sulcus; ITC: inferior temporal cortex; AUD: auditory cortex; aSTS: anterior superior temporal sulcus; mSTS: middle STS; pSTS: posterior STS; MT: middle temporal visual motion area; V4: visual area 4; V1-V2:primary and secondary visual cortices.

ent motion were not significantly affected by training history, in contrast to β oscillatory activity seemingly affected by the degree of integrated evidence during training. β oscillations may play an important role in (multi)sensory perceptual discrimination consistent with its role in mediating interactions across distant structures during perceptual decision-making [25]. To disentangle the possible networks mediating these effects, we turned to multivariate functional connectivity (FC) analysis and investigated whether medium- and long-range interactions between cortical regions could provide complementary insights on the specificity of oscillatory regimes as a function of sensory history in training (Figure 1.E).

3.5. Task-related network synchronization during visual coherent motion discrimination

To characterize the functional connectivity (FC) induced by (multi)sensory training in the different oscillatory regimes, we estimated the PRE and POST activity during the presentation of motion coherence (i.e., excluding the initial incoherence interval of the stimuli) using 28 cortical regions (ROIs; Figure 4.A). Hence, the bivariate FC was estimated using the weighted phase-lag index (wPLI) (Figure 4.A) in three main synchronization regimes (α, β and high γ). ROIs were selected in a manner orthogonal to the contrasts of interest, mainly by performing a source estimation of the grand average data across all experimental conditions ([17], see Methods). All statistical contrasts (Figure 4.B) were based on non-parametric permutation t-tests. Only phase coupling values showing significant differences ($p < 0.01$) were retained in the resulting functional networks herein reported.

First, we estimated the functional connectivity pattern during PRE and POST (*i.e.* during task), which significantly differed from resting-state (PRE *vs.* REST and POST *vs.* REST; Figure 4.B). The subtraction of the resting-state FC from PRE and POST was used as an equivalent of baseline in univariate analyses, and thus was performed to ensure that we characterized the task-relevant FC in both POST and PRE relative to the resting-state network. A direct comparison of POST *vs.* PRE FC without consideration of the initial resting-state FC would be a confounding factor in the interpretation of the results, and could falsely assign significant changes of FC to training effects, when they may in fact simply result from transitioning from REST to task. We then considered the task-relevant networks common to PRE and POST (Figure 4.C, top) and explored the effects of training on the changes of cortical interactions and oscillatory couplings.

Consistent with the occipital decrease in α band power observed in the univariate time-frequency analysis, we found a significant uncoupling of the α oscillatory network in task (both in PRE and in POST) as compared to REST (Figure 5.A, bottom left panel). A relative increase in synchronization modulated by sensory history (Figure 5.A, left column) was also found from PRE to POST, involving a large network comprising occipital, temporal and parietal regions. This relative significant increase in α synchronization was observed in the V and in the AV groups, but not in the CTRL group. A similar analysis was performed for the β and the γ oscillatory regimes. Contrary to the α desynchronization from REST to task (PRE, POST), the β and γ activiy showed a strengthening of large-scale

coupling between REST and task (PRE, POST) (Figure 5.A, bottom panels). The task-related β network present in all groups implicated vlPFC, IPS and MT but showed a significant strengthening from PRE to POST solely in the AV group (5.A, middle column). The significant relative increase of task-related FC (POST *vs.* PRE) was also observed for the AV group in the high γ regime implicating the auditory regions and the pSTS. In sum, all three groups displayed a characteristic desynchronization of the α network when engaged in the task, but a higher relative synchronization of the α network in POST as compared to PRE for the AV and V groups. Conversely, an increased synchronization of β and γ networks was found in all three groups from resting-state to task (PRE, POST), but only in the AV group did we see an increase of β and γ synchronization following training.

3.6. Brain network analysis and topological differences in regional connectivity

To investigate the degree of interaction of each brain region, a brain network analysis was carried out using a measure of centrality as index (cf Eq. (3)). This analysis allowed investigating whether specific regions played a central role by assessing the topology of the estimated FC networks based on the number of phase coupling values (connections) over a specific threshold for each ROI (*i.e.* node degree, see Experimental Procedures). This quantification revealed distinct patterns for each oscillatory regime (Figure 5.B), all corroborating our previous analyses (Figure 5.A). The changes in the node degree within the estimated FC networks were assessed with the statistical contrasts PRE *vs.* REST combining all groups, and POST *vs.* PRE on a per group basis.

First, a general task-related decrease of node degree from REST to PRE (Figure 5.B, α blue nodes, top left) was observed in parietal, occipital and temporal regions for the α oscillatory network. This observation was consistent with the global α desynchronization during task as compared to REST. The same contrast for the β network (Figure 5.B, β, top middle) showed an increase of node degree in PRE in frontal and parietal regions (red nodes), but a decrease in occipito-temporal regions (blue nodes) as compared to REST networks. This pattern was expected considering that long-range cortical interactions in the β band are known to involve fronto-parietal regions during perceptual decision-making [64, 25]. Motor cortices also showed a higher node degree in PRE than in REST, reflecting the information flow during task execution mediated by β oscillatory networks. The same contrast for the γ network (Figure 5.B, γ, top right) showed mainly a left-lateralized decrease of node degree but an increase in posterior regions.

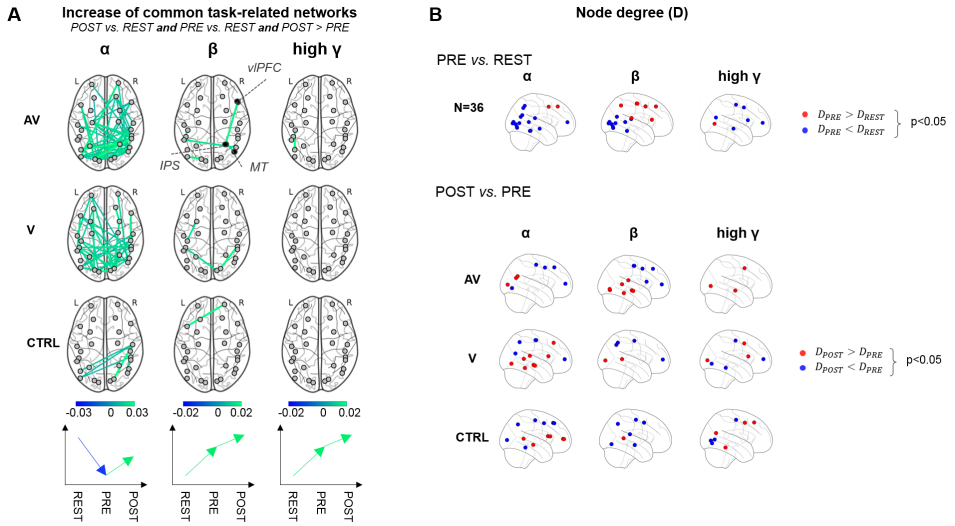

Figure 5: **Fluctuations of the task-related networks in PRE- and POST-training**. (**A**) Source estimation was performed to obtain cortical activity in 28 regions of interest (see Section 2.7 for details). Pairwise cortical interactions based on wPLI, and averaged in each frequency band of interest, were estimated for each condition (REST, PRE and POST). POST *vs.* PRE contrasts of cortical interactions (lines connecting two regions in the figure) within the task-related FC network common to PRE and POST were separately studied for α (left), β (middle), and γ (right) and for the 3 training groups (AV:top, V: middle; CTRL: bottom). A qualitative description of FC changes (significant increases and decreases of interactions) is provided at the bottom, showing that increases from PRE to POST were relative to REST, with an initial desynchronization of α from REST to task (POST,PRE), and a relative synchronization of β and γ from REST to task (POST,PRE) was found in all three groups. The AV and V groups showed a relative increase of α FC from PRE to POST. Although a significant β phase-coupling in task-related FC network linking IPS, vLPFC and MT was found in all groups, only the AV group showed a significant strengthening of the β network following training. (**B**) Topological changes in FC networks from REST to PRE (top) and from PRE to POST (bottom). POST *vs.* PRE contrasts were performed for each training group separately. In the β network, the node degree in PRE increased in frontal and parietal regions, whereas it decreased in occipito-temporal regions as compared to REST. The reverse pattern was observed in the β network from PRE to POST in the AV group. See also Inline Supp. Mat.C

We then investigated the changes in FC between POST and PRE as a function of training (Figure 5.B, bottom rows). For the AV group, the analysis of β oscillatory networks revealed a clear reversal of the node degree pattern in the POST *vs.* PRE contrast as compared to the PRE *vs.* REST contrast: an increase of node degree from PRE to POST was observed in occipito-temporal regions (mainly in the right hemisphere), while a decrease was found in frontal regions (mainly in the left hemisphere). The node degree value of β oscillatory networks implicating motor cortices also decreased with training in all three experimental groups. Conversely, the right mSTS region, which showed a decreasing node degree from REST to PRE, now consistently increased from PRE to POST in all three groups. This suggested the implication of the mSTS during actual training, the synchronization of which got stronger and more extensive (up to visual regions V4) following training.

In the topological analysis of high γ oscillatory networks, frontal regions exhibited opposite dynamics as compared to our observation in the β band. The node degree of the left frontal BA6 region (pre-motor and supplementary motor regions) decreased from REST to PRE, and increased from PRE to POST for the three groups. These results were in line with previous literature [64] showing that high γ and β choice-predictive activities showed opposite changes during perceptual decision-making. In the same study [64], oscillatory activities build up gradually during stimulus evidence encoding to reflect the integration of high γ activity in MT. Here, on the other hand, the node degree in mSTS and MT regions selectively increased after congruent multisensory training, consistent with the observed selective implication of these regions in the task [17].

3.7. Emergence of β and γ functional networks following training with coherent audiovisual motion

The potential emergence of new functional coupling of cortical brain networks following training (*i.e.*, POST-specific) was addressed on a per group basis (Figure 4.C, bottom). In Figure 6.A, we report cortical interactions that were specific to post-training, *i.e.*, phase couplings among brain regions that were not significantly seen in the PRE *vs.* REST contrast but which significantly emerged after training in the POST *vs* REST contrast (see Methods). The POST-specific couplings between cortical regions emerged in a training-selective manner in the β band and only for the AV training group (Figure 6.A). This suggested that multisensory training with temporally comodulated audiovisual stimuli could subsequently affect the organization of cortical interactions during a purely visual discrimination

task. The observed reorganization notably encompassed long-range interactions in POST-specific networks around temporal cortices, consistent with the results of the topological analysis shown in Figure 5.B. Additionally, the emergence of high γ phase-coupling after training was found mainly in the AV and the V training groups, while POST-specific α connectivity emerged in the CTRL group. Intriguingly, the sole behavioral variable relevant to the emergence of the β connectivity was participants' confidence ratings: a significant linear correlation ($N = 12$, $r = 0.72$, $p = 0.011$) was observed so that an increase in POST-specific β band connectivity solely observed in the AV group was commensurate with an increase in these participants' confidence ratings on the task.

4. Discussion

In this study, we asked how internalized content, established on the basis of temporally coherent audiovisual signals, subsequently benefit the discrimination of visual motion coherence. During the presentation of visual motion stimuli, the spectral signatures of brain responses included a decrease in occipital α and frontal β power, and an increase of occipital γ power. While the occipital γ correlated with the strength in visual motion coherence and the post-training performance, α activity showed no functional modulation as a function of stimulus property, sensory evidence, performance or training. Additionally, several contrasts revealed that the local β power captured an integrated aspect of evidence based decision-making as a function of training history. Second, multivariate functional connectivity analysis based on oscillatory phase coupling showed a relative global increase of α ($8-14$ Hz) phase synchronization post-training in the V and AV groups as compared to the CTRL group; this was found in the context of a general decrease of α FC as compared to REST. Third, and importantly, we report the emergence of long-range β ($15-30$ Hz) and γ ($60-120$ Hz) synchronization networks implicating temporal, prefrontal, parietal and visual cortices. The emergence of the β and γ networks was essentially observed following congruent (but not incongruent) multisensory training and the β network was indicative of participants' confidence rating in post-training. Despite the limit represented by the number of participants in this study ($N = 36$), altogether, our results suggest that sensory history in training can subsequently strengthen decision-making networks through the regulation of large-scale oscillatory synchronizations. It would thus be beneficial in the future to increase the number of participants for robust estimation of network changes and characterization. It would also be interesting to test whether similar pattern of

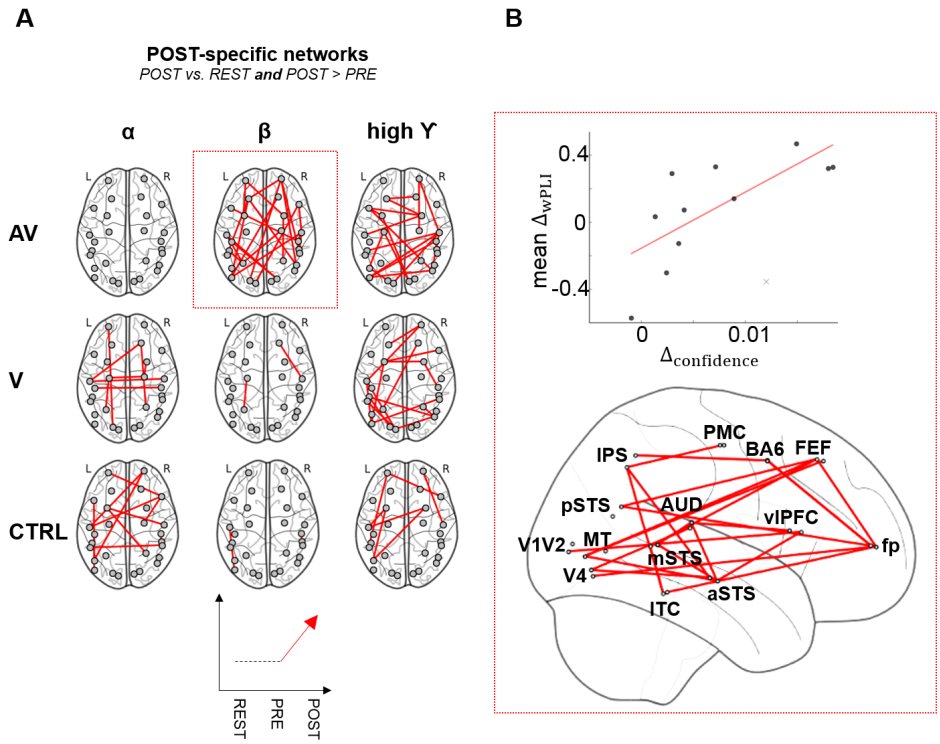

Figure 6: **Emerging oscillatory networks following training**. (**A**) The phase synchronization based on pairwise wPLI between brain regions (lines connecting two regions in the figure) in α, β, and γ oscillatory regimes was investigated separately as a function of training group. The central finding was the emergence of novel mid- to long-range cortical interactions (POST-specific network, not present during PRE) in the β and γ networks especially in the AV group. The CTRL group trained with incongruent AV stimuli showed the largest synchronization in α. (**B**) A linear correlation between the average increase of the β band POST-specific interactions from PRE to POST and the increase in participants' confidence ratings was observed solely for the AV group (top panel). The β band POST-specific network was mainly characterized by fronto-occipital and temporo-parietal interactions (bottom panel).

beta network can be seen in sensory-impaired populations. The patterns observed in the present study arose from a selected number of cortical regions of interest investigated, which represent a second limit to overcome in future research.

4.1. Interplay between top-down α and feedforward γ

Attending stimuli increases both the local and large-scale synchronization of rhythmic neuronal activity in the γ band [78, 79, 80, 81, 82]. An increase γ power has been reported during binding ([83, 84]), multisensory integration [85, 86] and semantic congruence across sensory modalities [87, 88]. Here, we observed an increase in occipital high γ band during the presentation of visual motion which, consistent with previous work [89, 38, 25], increased with increasing strength in visual motion coherence. This effect was seen in visual cortices for all three experimental groups, both before and after their respective training. This pattern converged with the notion that γ power provides a spectral index of sensory evidence encoding [38, 25], and here, may further be a significant indicator of participants' correct perceptual discrimination following training. As expected [79, 90, 91, 66], we also observed a concomitant decrease in occipital α power. Seminal work has suggested that α suppression was stronger for the detection of meaningful objects than for scrambled ones [92], and associated with visuo-spatial [93] and object-based [68] selective attention. An increase in pre-stimulus α power is also known to impair detection [94, 95, 96, 97, 98, 99, 100] and, conversely, an increase in α power is often observed in unattended modalities [101, 102, 103]. α oscillations are deemed instrumental for selective attention and the top-down control of information ([104]). The modulation of occipital α was previously shown to correlate with behavioral improvements of visual motion discrimination in presence of congruently moving sounds [105]. Here, no systematic changes in the occipital α were found as a function of experimental or behavioral variables, and this was likely due to differences in paradigmatic and methodological approaches: the most notable one being that we did not directly contrast unisensory *vs* multisensory stimulations *per se*. Rather, the stable level of occipital α power over experimental conditions parsimoniously indicated that all participants were effectively attentive to the stimuli irrespective of the strength of motion coherence or training history. Recent work has also suggested that γ and α (and β) activity were markers of feedforward and feedback propagation, respectively [106, 81, 107, 108, 109, 110, 111, 112]. Given the pattern of stable α suppression and increased γ power as a function of motion coherence (and post-training correctness), one possible working hypothesis is

that, given a stable and sustained endogenous attentional control exerted in the α range, perceptual training may improve the efficiency with which γ activity propagates sensory evidence up the hierarchy.

4.2. The effect of sensory history in training on α and γ network phase-synchronization

In line with the notion that α oscillations actively contribute to the selection of cortical regions during task [113, 114], a decrease of global α phase synchronization was observed from resting-state (REST) to task (PRE, POST) in all groups. Yet, and perhaps more importantly, a relative global increase in α synchronization engaging a parieto-occipital network was observed in post-training as compared to pre-training in both the AV and V groups. This pattern was interestingly not observed in the CTRL group, who was trained with distracting uncorrelated sounds. Rather, the CTRL group (and to some extent, the V group) showed a fronto-parietal α synchronization post-training. The presence of large-scale α synchronization in the CTRL group could be primarily explained by the selective function of α networks, which may help decouple brain regions during conflicting inputs (CTRL). Specifically, at the same time we observed these patterns in the α FC, we also observed a global strengthening of the post-training γ synchronization network. γ-band synchronization in brain networks is fundamental in cortical communication as phase-coupling across brain regions may promote the transmission of information across large-scale neuronal networks [90, 82, 109]. Global γ synchronization is notably considered to denote "*effective, precise and selective*" communication [82]). In this study, training may have improved long-range γ synchronization with a possible gain in communication efficiency consistent with the general improvement on the task observed in all groups [17]. Sensory history in training affected the general increase of γ phase synchronization so that the group with the largest behavioral improvement, *i.e.* the AV group, also showed the strongest increase followed by the V and the CTRL group. Altogether, theses results suggest that the type of sensory inputs during a very short training (here a total of 20 minutes) can selectivity affect the coordination of brain regions implicated in the endogenous control of information processing.

4.3. β oscillations as integrated evidence

Very recently, β oscillations have been proposed to be markers of internal content [26] and supramodal processing [27]: following learning, rhythms

such as β oscillations may regulate the feedback processing of sensory analysis [115] based on abstract categorical representations. These internal network dynamics were observed in prefrontal cortices, and operated in the α/β bands [115]. An important finding in our study is the fundamental role of β oscillations, both as local power decrease during sensory encoding and decision-making in all groups, and as an emergent large-scale network following congruent multisensory AV training. Several studies have reported an increased coherence or synchronization in the β band associated with multisensory stimulation [116, 117] and, consistent with the implication of the β band in sensorimotor processing [24], β activity was related to participants response speed in multisensory context. Gleiss and Kayser [118] reported early differences in β band activity but did not find any correlation with behavior. Consistent with another study [117], we found that local modulations of β power were observed when participants were engaged in the task but not during passive viewing, and that RT was the main contributor for this effect: the decrease in local β power was found for contrasts in which evidence-based decisions were most successful (*i.e.*, for strongest as compared to weakest visual motion coherence, for correct as compared to incorrect trials and for post- compared to pre-training trials). Under the working hypothesis that abstract internal content [115, 33] has been learned to drive the processing of incoming sensory information, the strengthening of the large-scale β coupling in the group that has received congruent AV training would further suggest that performing the task with temporally coherent audiovisual events strengthened the ability to predict motion coherence in vision. In other words, the changes in β power and network synchronization may capture endogenous top-down activations of task-relevant (supramodal) cortical representations, which facilitate communication between brain regions [119, 25, 26, 27, 28].

In this context, recent predictive coding models drawing from audiovisual speech processing [11, 14, 120] and neurophysiological work [112, 28] have pushed forward the notion that prediction errors from one sensory modality to another may be communicated in the γ range, whereas top-down predictions may be mediated by β oscillations [120]. As the emergent β network was solely seen for the AV group in which it was linearly related to confidence rating, we speculate that the hypothesized combined effects of increased communication efficiency in a feedfoward γ network, the endogenous selective routing in the α network, and the predictive β propagation in the AV group may all contribute to the local selective changes previously reported in the human motion area MT as a change in the neurometric threshold [17]. The notion that internal content (as supramodal or abstract

representations) may constrain sensory analysis early on provides additional evidence for the implication of large-scale neural oscillations in integrative and predictive brain functions.

4.4. Limitations

It is perhaps noteworthy that our γ-band results do not necessarily imply nor preclude the presence of underlying oscillatory sources. Several studies have cast doubt on the idea that task-related changes or ongoing background activity in γ-band dynamics are consistently due to oscillations [121, 122, 123]. Accordingly, the power spectrum does not always show a distinct peak that could unequivocally index oscillations. Instead broad-band power changes are often observed that may exhibit 1/f scale-free behavior [124] and may be accounted for in terms of short-lived stochastic spiking [125]. We want to emphasize that our study does not possess the requisite statistical power or experimental paradigm to tell apart these concurrent interpretations. We, therefore, carefully suggest to view our γ–band findings as neuronal activity in the wider sense, leaving open the precise physiological generative mechanism. Our phase-based analysis in the γ-band may therefore suffer from specificity, and has to be regarded as pragmatic approximation that may get revised in the future upon the availability of more precise computational tools and an extended study-design.

4.5. Conclusion

Taken together, our results support the notion that cortical computations encompass sensory-based processing and that, consistent with the role of prefrontal cortices shifting activity from feedforward inputs to internal dynamics [115], the internal content shaped by multisensory inputs during short training can strengthen the selectivity of large-scale oscillatory networks for later adaptive purposes.

Acknowledgments

This work was supported by ANR-16-CE33-0020 MultiFracs, France, and the Marie Curie IRG-249222 and the ERC-YStG-263584 to V.vW. We thank Dr Laetitia Grabot, Dr Sophie Herbst, and Dr Tadeusz Kononowicz for their comments on the initial version of the MS.

[1] C. V. Parise, C. Spence, M. O. Ernst, When correlation implies causation in multisensory integration, Current Biology 22 (2012) 46–49.

[2] C. V. Parise, M. O. Ernst, Correlation detection as a general mechanism for multisensory integration, Nature communications 7 (2016).

[3] O. Deroy, C. Spence, U. Noppeney, Metacognition in multisensory perception, Trends in cognitive sciences 20 (2016) 736–747.

[4] C. Kayser, L. Shams, Multisensory causal inference in the brain, PLoS biology 13 (2015) e1002075.

[5] T. Rohe, U. Noppeney, Cortical hierarchies perform bayesian causal inference in multisensory perception, PLoS Biology 13 (2015) e1002073.

[6] Y. Cao, C. Summerfield, H. Park, B. L. Giordano, C. Kayser, Causal inference in the multisensory brain, Neuron (2019).

[7] N. W. Roach, J. Heron, P. V. McGraw, Resolving multisensory conflict: a strategy for balancing the costs and benefits of audio-visual integration, Proceedings of the Royal Society of London B: Biological Sciences 273 (2006) 2159–2168.

[8] C. Spence, Crossmodal correspondences: A tutorial review, Attention, Perception, & Psychophysics 73 (2011) 971–995.

[9] R. K. Maddox, H. Atilgan, J. K. Bizley, A. K. Lee, Auditory selective attention is enhanced by a task-irrelevant temporally coherent visual stimulus in human listeners, Elife 4 (2015).

[10] K. W. Grant, P.-F. Seitz, The use of visible speech cues for improving auditory detection of spoken sentences, The Journal of the Acoustical Society of America 108 (2000) 1197–1208.

[11] V. Van Wassenhove, K. W. Grant, D. Poeppel, Visual speech speeds up the neural processing of auditory speech, Proceedings of the National Academy of Sciences of the United States of America 102 (2005) 1181–1186.

[12] C. E. Schroeder, P. Lakatos, Y. Kajikawa, S. Partan, A. Puce, Neuronal oscillations and visual amplification of speech, Trends in cognitive sciences 12 (2008) 106–113.

[13] O. Nahorna, F. Berthommier, J.-L. Schwartz, Audio-visual speech scene analysis: characterization of the dynamics of unbinding and rebinding the mcgurk effect, The Journal of the Acoustical Society of America 137 (2015) 362–377.

[14] V. van Wassenhove, Speech through ears and eyes: interfacing the senses with the supramodal brain, Frontiers in psychology 4 (2013) 388.

[15] E. Van der Burg, C. N. Olivers, A. W. Bronkhorst, J. Theeuwes, Pip and pop: nonspatial auditory signals improve spatial visual search., Journal of Experimental Psychology: Human Perception and Performance 34 (2008) 1053.

[16] A. Kösem, V. Van Wassenhove, Temporal structure in audiovisual sensory selection, PLoS One 7 (2012) e40936.

[17] N. Zilber, P. Ciuciu, A. Gramfort, L. Azizi, V. Van Wassenhove, Supramodal processing optimizes visual perceptual learning and plasticity, Neuroimage 93 (2014) 32–46.

[18] D. Senkowski, T. R. Schneider, J. J. Foxe, A. K. Engel, Crossmodal binding through neural coherence: implications for multisensory processing, Trends in neurosciences 31 (2008) 401–409.

[19] J. Keil, D. Senkowski, Neural oscillations orchestrate multisensory processing, The Neuroscientist (2018) 1073858418755352.

[20] J. F. Hipp, A. K. Engel, M. Siegel, Oscillatory synchronization in large-scale cortical networks predicts perception, Neuron 69 (2011) 387–396.

[21] P. Lakatos, G. Karmos, A. D. Mehta, I. Ulbert, C. E. Schroeder, Entrainment of neuronal oscillations as a mechanism of attentional selection, science 320 (2008) 110–113.

[22] N. van Atteveldt, M. M. Murray, G. Thut, C. E. Schroeder, Multisensory integration: flexible use of general operations, Neuron 81 (2014) 1240–1253.

[23] J. K. Bizley, R. K. Maddox, A. K. Lee, Defining auditory-visual objects: Behavioral tests and physiological mechanisms, Trends in neurosciences 39 (2016) 74–85.

[24] A. K. Engel, P. Fries, Beta-band oscillationssignalling the status quo?, Current opinion in neurobiology 20 (2010) 156–165.

[25] M. Siegel, A. K. Engel, T. H. Donner, Cortical network dynamics of perceptual decision-making in the human brain, Frontiers in human neuroscience 5 (2011) 21.

[26] B. Spitzer, S. Haegens, Beyond the status quo: A role for beta oscillations in endogenous content (re) activation, Eneuro 4 (2017) ENEURO–0170.

[27] S. Haegens, J. Vergara, R. Rossi-Pool, L. Lemus, R. Romo, Beta oscillations reflect supramodal information during perceptual judgment, Proceedings of the National Academy of Sciences (2017) 201714633.

[28] S. L. Bressler, C. G. Richter, Interareal oscillatory synchronization in top-down neocortical processing, Current opinion in neurobiology 31 (2015) 62–66.

[29] M. Vinck, R. Oostenveld, M. Van Wingerden, F. Battaglia, C. M. Pennartz, An improved index of phase-synchronization for electrophysiological data in the presence of volume-conduction, noise and sample-size bias, Neuroimage 55 (2011) 1548–1565.

[30] L. M. Romanski, Representation and integration of auditory and visual stimuli in the primate ventral lateral prefrontal cortex, Cerebral Cortex 17 (2007) i61–i69.

[31] L. Romanski, J. Hwang, Timing of audiovisual inputs to the prefrontal cortex and multisensory integration, Neuroscience 214 (2012) 36–48.

[32] L. M. Romanski, Integration of faces and vocalizations in ventral prefrontal cortex: implications for the evolution of audiovisual speech, Proceedings of the National Academy of Sciences 109 (2012) 10717–10724.

[33] A. Wutz, R. Loonis, J. E. Roy, J. A. Donoghue, E. K. Miller, Different levels of category abstraction by different dynamics in different prefrontal areas, Neuron 97 (2018) 716–726.

[34] R. A. Andersen, Multimodal integration for the representation of space in the posterior parietal cortex, Philosophical Transactions of the Royal Society of London B: Biological Sciences 352 (1997) 1421–1428.

[35] N. Bolognini, A. Maravita, Uncovering multisensory processing through non-invasive brain stimulation, Frontiers in psychology 2 (2011).

[36] S. Pasalar, T. Ro, M. S. Beauchamp, Tms of posterior parietal cortex disrupts visual tactile multisensory integration, European Journal of Neuroscience 31 (2010) 1783–1790.

[37] T. H. Donner, M. Siegel, P. Fries, A. K. Engel, Buildup of choice-predictive activity in human motor cortex during perceptual decision making, Current Biology 19 (2009) 1581–1585.

[38] M. Siegel, T. H. Donner, R. Oostenveld, P. Fries, A. K. Engel, High-frequency activity in human visual cortex is modulated by visual motion strength, Cerebral Cortex 17 (2006) 732–741.

[39] P. B. Meijer, An experimental system for auditory image representations, IEEE transactions on biomedical engineering 39 (1992) 112–121.

[40] S. Levy-Tzedek, S. Hanassy, S. Abboud, S. Maidenbaum, A. Amedi, Fast, accurate reaching movements with a visual-to-auditory sensory substitution device, Restorative neurology and neuroscience 30 (2012) 313–323.

[41] R. D. Melara, T. P. O'brien, Interaction between synesthetically corresponding dimensions., Journal of Experimental Psychology: General 116 (1987) 323.

[42] F. Maeda, R. Kanai, S. Shimojo, Changing pitch induced visual motion illusion, Current biology 14 (2004) R990–R991.

[43] T. Overath, S. Kumar, L. Stewart, K. von Kriegstein, R. Cusack, A. Rees, T. D. Griffiths, Cortical mechanisms for the segregation and representation of acoustic textures, Journal of Neuroscience 30 (2010) 2070–2076.

[44] A. Gramfort, M. Luessi, E. Larson, D. A. Engemann, D. Strohmeier, C. Brodbeck, L. Parkkonen, M. S. Hämäläinen, Mne software for processing meg and eeg data, Neuroimage 86 (2014) 446–460.

[45] A. Gramfort, M. Luessi, E. Larson, D. A. Engemann, D. Strohmeier, C. Brodbeck, R. Goj, M. Jas, T. Brooks, L. Parkkonen, et al., Meg and eeg data analysis with mne-python, Frontiers in neuroscience 7 (2013) 267.

[46] J. Gross, S. Baillet, G. R. Barnes, R. N. Henson, A. Hillebrand, O. Jensen, K. Jerbi, V. Litvak, B. Maess, R. Oostenveld, et al., Good

practice for conducting and reporting meg research, Neuroimage 65 (2013) 349–363.

[47] S. Taulu, J. Simola, Spatiotemporal signal space separation method for rejecting nearby interference in meg measurements, Physics in medicine and biology 51 (2006) 1759.

[48] E. Maris, R. Oostenveld, Nonparametric statistical testing of eeg-and meg-data, Journal of neuroscience methods 164 (2007) 177–190.

[49] M. J. Anderson, P. Legendre, An empirical comparison of permutation methods for tests of partial regression coefficients in a linear model, Journal of statistical computation and simulation 62 (1999) 271–303.

[50] C. J. DiCiccio, J. P. Romano, Robust permutation tests for correlation and regression coefficients, Journal of the American Statistical Association (2017) 1–10.

[51] A. M. Winkler, G. R. Ridgway, M. A. Webster, S. M. Smith, T. E. Nichols, Permutation inference for the general linear model, Neuroimage 92 (2014) 381–397.

[52] A. M. Dale, A. K. Liu, B. R. Fischl, R. L. Buckner, J. W. Belliveau, J. D. Lewine, E. Halgren, Dynamic statistical parametric mapping: combining fmri and meg for high-resolution imaging of cortical activity, Neuron 26 (2000) 55–67.

[53] S.-R. Farahibozorg, R. N. Henson, O. Hauk, Adaptive cortical parcellations for source reconstructed eeg/meg connectomes, NeuroImage 169 (2018) 23–45.

[54] G. L. Colclough, M. W. Woolrich, P. Tewarie, M. J. Brookes, A. J. Quinn, S. M. Smith, How reliable are meg resting-state connectivity metrics?, Neuroimage 138 (2016) 284–293.

[55] S. Khan, J. A. Hashmi, F. Mamashli, K. Michmizos, M. G. Kitzbichler, H. Bharadwaj, Y. Bekhti, S. Ganesan, K.-L. A. Garel, S. Whitfield-Gabrieli, et al., Maturation trajectories of cortical resting-state networks depend on the mediating frequency band, NeuroImage 174 (2018) 57–68.

[56] M. Jas, E. Larson, D. A. Engemann, J. Leppäkangas, S. Taulu, M. Hämäläinen, A. Gramfort, A reproducible meg/eeg group study

with the mne software: recommendations, quality assessments, and good practices, Frontiers in neuroscience 12 (2018).

[57] R. S. Desikan, F. Ségonne, B. Fischl, B. T. Quinn, B. C. Dickerson, D. Blacker, R. L. Buckner, A. M. Dale, R. P. Maguire, B. T. Hyman, et al., An automated labeling system for subdividing the human cerebral cortex on mri scans into gyral based regions of interest, Neuroimage 31 (2006) 968–980.

[58] K. Ansari-Asl, L. Senhadji, J.-J. Bellanger, F. Wendling, Quantitative evaluation of linear and nonlinear methods characterizing interdependencies between brain signals, Physical Review E 74 (2006) 031916.

[59] C. J. Stam, G. Nolte, A. Daffertshofer, Phase lag index: assessment of functional connectivity from multi channel eeg and meg with diminished bias from common sources, Human brain mapping 28 (2007) 1178–1193.

[60] A. V. Sazonov, C. K. Ho, J. W. Bergmans, J. B. Arends, P. A. Griep, E. A. Verbitskiy, P. J. Cluitmans, P. A. Boon, An investigation of the phase locking index for measuring of interdependency of cortical source signals recorded in the eeg, Biological cybernetics 100 (2009) 129.

[61] F. De Vico Fallani, J. Richiardi, M. Chavez, S. Achard, Graph analysis of functional brain networks: practical issues in translational neuroscience, Phil. Trans. R. Soc. B 369 (2014) 20130521.

[62] E. Bullmore, O. Sporns, Complex brain networks: graph theoretical analysis of structural and functional systems, Nature Reviews Neuroscience 10 (2009) 186–198.

[63] F. De Vico Fallani, V. Latora, M. Chavez, A topological criterion for filtering information in complex brain networks, PLoS computational biology 13 (2017) e1005305.

[64] T. H. Donner, M. Siegel, R. Oostenveld, P. Fries, M. Bauer, A. K. Engel, Population activity in the human dorsal pathway predicts the accuracy of visual motion detection, Journal of Neurophysiology 98 (2007) 345–359.

[65] J. B. Swettenham, S. D. Muthukumaraswamy, K. D. Singh, Spectral properties of induced and evoked gamma oscillations in human early

visual cortex to moving and stationary stimuli, Journal of neurophysiology 102 (2009) 1241–1253.

[66] O. Jensen, A. Mazaheri, Shaping functional architecture by oscillatory alpha activity: gating by inhibition, Frontiers in human neuroscience 4 (2010) 186.

[67] J. M. Zumer, R. Scheeringa, J.-M. Schoffelen, D. G. Norris, O. Jensen, Occipital alpha activity during stimulus processing gates the information flow to object-selective cortex, PLoS biology 12 (2014) e1001965.

[68] J. J. Foxe, A. C. Snyder, The role of alpha-band brain oscillations as a sensory suppression mechanism during selective attention, Frontiers in psychology 2 (2011) 154.

[69] A. Von Stein, J. Sarnthein, Different frequencies for different scales of cortical integration: from local gamma to long range alpha/theta synchronization, International journal of psychophysiology 38 (2000) 301–313.

[70] M. Alavash, C. Daube, M. Woestmann, A. Brandmeyer, J. Obleser, Large-scale network dynamics of beta-band oscillations underlie auditory perceptual decision-making, Network Neuroscience 1 (2017) 166–191.

[71] M. Saleh, J. Reimer, R. Penn, C. L. Ojakangas, N. G. Hatsopoulos, Fast and slow oscillations in human primary motor cortex predict oncoming behaviorally relevant cues, Neuron 65 (2010) 461–471.

[72] F. Cassim, C. Monaca, W. Szurhaj, J.-L. Bourriez, L. Defebvre, P. Derambure, J.-D. Guieu, Does post-movement beta synchronization reflect an idling motor cortex?, Neuroreport 12 (2001) 3859–3863.

[73] M. Bauer, S. Kennett, J. Driver, Attentional selection of location and modality in vision and touch modulates low-frequency activity in associated sensory cortices, Journal of neurophysiology 107 (2012) 2342–2351.

[74] G. Pfurtscheller, F. L. Da Silva, Event-related eeg/meg synchronization and desynchronization: basic principles, Clinical neurophysiology 110 (1999) 1842–1857.

[75] T. Mima, N. Simpkins, T. Oluwatimilehin, M. Hallett, Force level modulates human cortical oscillatory activities, Neuroscience letters 275 (1999) 77–80.

[76] N. Jenkinson, P. Brown, New insights into the relationship between dopamine, beta oscillations and motor function, Trends in neurosciences 34 (2011) 611–618.

[77] V. Wyart, V. De Gardelle, J. Scholl, C. Summerfield, Rhythmic fluctuations in evidence accumulation during decision making in the human brain, Neuron 76 (2012) 847–858.

[78] A. K. Engel, P. Fries, W. Singer, Dynamic predictions: oscillations and synchrony in top–down processing, Nature Reviews Neuroscience 2 (2001) 704.

[79] P. Fries, J. H. Reynolds, A. E. Rorie, R. Desimone, Modulation of oscillatory neuronal synchronization by selective visual attention, Science 291 (2001) 1560–1563.

[80] F. Varela, J.-P. Lachaux, E. Rodriguez, J. Martinerie, The brainweb: phase synchronization and large-scale integration, Nature reviews neuroscience 2 (2001) 229.

[81] X.-J. Wang, Neurophysiological and computational principles of cortical rhythms in cognition, Physiological reviews 90 (2010) 1195–1268.

[82] P. Fries, Rhythms for cognition: communication through coherence, Neuron 88 (2015) 220–235.

[83] W. Singer, C. M. Gray, Visual feature integration and the temporal correlation hypothesis, Annual review of neuroscience 18 (1995) 555–586.

[84] P. Fries, P. R. Roelfsema, A. K. Engel, P. König, W. Singer, Synchronization of oscillatory responses in visual cortex correlates with perception in interocular rivalry, Proceedings of the National Academy of Sciences 94 (1997) 12699–12704.

[85] J. Bhattacharya, L. Shams, S. Shimojo, Sound-induced illusory flash perception: role of gamma band responses, Neuroreport 13 (2002) 1727–1730.

[86] J. Mishra, A. Martinez, T. J. Sejnowski, S. A. Hillyard, Early cross-modal interactions in auditory and visual cortex underlie a sound-induced visual illusion, Journal of Neuroscience 27 (2007) 4120–4131.

[87] S. Yuval-Greenberg, L. Y. Deouell, What you see is not (always) what you hear: induced gamma band responses reflect cross-modal interactions in familiar object recognition, Journal of Neuroscience 27 (2007) 1090–1096.

[88] T. R. Schneider, S. Debener, R. Oostenveld, A. K. Engel, Enhanced eeg gamma-band activity reflects multisensory semantic matching in visual-to-auditory object priming, Neuroimage 42 (2008) 1244–1254.

[89] A. Sokolov, W. Lutzenberger, M. Pavlova, H. Preissl, C. Braun, N. Birbaumer, Gamma-band meg activity to coherent motion depends on task-driven attention, Neuroreport 10 (1999) 1997–2000.

[90] P. Fries, Neuronal gamma-band synchronization as a fundamental process in cortical computation, Annual review of neuroscience 32 (2009) 209–224.

[91] M. Siegel, T. H. Donner, A. K. Engel, Spectral fingerprints of large-scale neuronal interactions, Nature Reviews Neuroscience 13 (2012) 121.

[92] S. Vanni, A. Revonsuo, R. Hari, Modulation of the parieto-occipital alpha rhythm during object detection, Journal of Neuroscience 17 (1997) 7141–7147.

[93] P. Sauseng, W. Klimesch, W. Stadler, M. Schabus, M. Doppelmayr, S. Hanslmayr, W. R. Gruber, N. Birbaumer, A shift of visual spatial attention is selectively associated with human eeg alpha activity, European Journal of Neuroscience 22 (2005) 2917–2926.

[94] N. A. Busch, J. Dubois, R. VanRullen, The phase of ongoing eeg oscillations predicts visual perception, Journal of Neuroscience 29 (2009) 7869–7876.

[95] H. Van Dijk, J.-M. Schoffelen, R. Oostenveld, O. Jensen, Prestimulus oscillatory activity in the alpha band predicts visual discrimination ability, Journal of Neuroscience 28 (2008) 1816–1823.

[96] S. Hanslmayr, A. Aslan, T. Staudigl, W. Klimesch, C. S. Herrmann, K.-H. Bäuml, Prestimulus oscillations predict visual perception performance between and within subjects, Neuroimage 37 (2007) 1465–1473.

[97] S. Haegens, B. F. Händel, O. Jensen, Top-down controlled alpha band activity in somatosensory areas determines behavioral performance in a discrimination task, Journal of Neuroscience 31 (2011) 5197–5204.

[98] S. R. Jones, C. E. Kerr, Q. Wan, D. L. Pritchett, M. Hämäläinen, C. I. Moore, Cued spatial attention drives functionally relevant modulation of the mu rhythm in primary somatosensory cortex, Journal of Neuroscience 30 (2010) 13760–13765.

[99] Y. Zhang, M. Ding, Detection of a weak somatosensory stimulus: Role of the prestimulus mu rhythm and its top–down modulation, Journal of cognitive neuroscience 22 (2010) 307–322.

[100] L. Grabot, A. Kösem, L. Azizi, V. van Wassenhove, Prestimulus alpha oscillations and the temporal sequencing of audiovisual events, Journal of cognitive neuroscience 29 (2017) 1566–1582.

[101] N. A. Busch, R. VanRullen, Spontaneous eeg oscillations reveal periodic sampling of visual attention, Proceedings of the National Academy of Sciences 107 (2010) 16048–16053.

[102] S. P. Kelly, E. C. Lalor, R. B. Reilly, J. J. Foxe, Increases in alpha oscillatory power reflect an active retinotopic mechanism for distracter suppression during sustained visuospatial attention, Journal of neurophysiology 95 (2006) 3844–3851.

[103] M. S. Worden, J. J. Foxe, N. Wang, G. V. Simpson, Anticipatory biasing of visuospatial attention indexed by retinotopically specific-band electroencephalography increases over occipital cortex, J Neurosci 20 (2000) 1–6.

[104] S. Sadaghiani, A. Kleinschmidt, Brain networks and α-oscillations: structural and functional foundations of cognitive control, Trends in cognitive sciences 20 (2016) 805–817.

[105] S. Gleiss, C. Kayser, Oscillatory mechanisms underlying the enhancement of visual motion perception by multisensory congruency, Neuropsychologia 53 (2014) 84–93.

[106] T. Van Kerkoerle, M. W. Self, B. Dagnino, M.-A. Gariel-Mathis, J. Poort, C. Van Der Togt, P. R. Roelfsema, Alpha and gamma oscillations characterize feedback and feedforward processing in monkey visual cortex, Proceedings of the National Academy of Sciences 111 (2014) 14332–14341.

[107] J. H. Lee, M. A. Whittington, N. J. Kopell, Top-down beta rhythms support selective attention via interlaminar interaction: a model, PLoS computational biology 9 (2013) e1003164.

[108] A. M. Bastos, W. M. Usrey, R. A. Adams, G. R. Mangun, P. Fries, K. J. Friston, Canonical microcircuits for predictive coding, Neuron 76 (2012) 695–711.

[109] A. M. Bastos, J. Vezoli, C. A. Bosman, J.-M. Schoffelen, R. Oostenveld, J. R. Dowdall, P. De Weerd, H. Kennedy, P. Fries, Visual areas exert feedforward and feedback influences through distinct frequency channels, Neuron 85 (2015) 390–401.

[110] E. A. Buffalo, P. Fries, R. Landman, T. J. Buschman, R. Desimone, Laminar differences in gamma and alpha coherence in the ventral stream, Proceedings of the National Academy of Sciences 108 (2011) 11262–11267.

[111] G. Michalareas, J. Vezoli, S. Van Pelt, J.-M. Schoffelen, H. Kennedy, P. Fries, Alpha-beta and gamma rhythms subserve feedback and feedforward influences among human visual cortical areas, Neuron 89 (2016) 384–397.

[112] C. G. Richter, W. H. Thompson, C. A. Bosman, P. Fries, Top-down beta enhances bottom-up gamma, Journal of Neuroscience 37 (2017) 6698–6711.

[113] S. Palva, J. M. Palva, Functional roles of alpha-band phase synchronization in local and large-scale cortical networks, Frontiers in psychology 2 (2011) 204.

[114] S. Palva, J. M. Palva, New vistas for α-frequency band oscillations, Trends in neurosciences 30 (2007) 150–158.

[115] S. L. Brincat, E. K. Miller, Prefrontal cortex networks shift from external to internal modes during learning, Journal of Neuroscience 36 (2016) 9739–9754.

[116] A. von Stein, P. Rappelsberger, J. Sarnthein, H. Petsche, Synchronization between temporal and parietal cortex during multimodal object processing in man, Cerebral Cortex 9 (1999) 137–150.

[117] M. R. Mercier, S. Molholm, I. C. Fiebelkorn, J. S. Butler, T. H. Schwartz, J. J. Foxe, Neuro-oscillatory phase alignment drives speeded multisensory response times: an electro-corticographic investigation, Journal of Neuroscience 35 (2015) 8546–8557.

[118] S. Gleiss, C. Kayser, Oscillatory mechanisms underlying the enhancement of visual motion perception by multisensory congruency, Neuropsychologia 53 (2014) 84–93.

[119] N. Kopell, G. Ermentrout, M. Whittington, R. Traub, Gamma rhythms and beta rhythms have different synchronization properties, Proceedings of the National Academy of Sciences 97 (2000) 1867–1872.

[120] L. H. Arnal, V. Wyart, A.-L. Giraud, Transitions in neural oscillations reflect prediction errors generated in audiovisual speech, Nature neuroscience 14 (2011) 797.

[121] S. Ray, J. H. Maunsell, Different origins of gamma rhythm and high-gamma activity in macaque visual cortex, PLoS biology 9 (2011) e1000610.

[122] J. R. Manning, J. Jacobs, I. Fried, M. J. Kahana, Broadband shifts in local field potential power spectra are correlated with single-neuron spiking in humans, Journal of Neuroscience 29 (2009) 13613–13620.

[123] R. Scheffer-Teixeira, H. Belchior, R. N. Leao, S. Ribeiro, A. B. Tort, On high-frequency field oscillations (¿ 100 hz) and the spectral leakage of spiking activity, Journal of Neuroscience 33 (2013) 1535–1539.

[124] B. Voytek, M. A. Kramer, J. Case, K. Q. Lepage, Z. R. Tempesta, R. T. Knight, A. Gazzaley, Age-related changes in 1/f neural electrophysiological noise, Journal of Neuroscience 35 (2015) 13257–13265.

[125] K. J. Miller, C. J. Honey, D. Hermes, R. P. Rao, J. G. Ojemann, et al., Broadband changes in the cortical surface potential track activation of functionally diverse neuronal populations, Neuroimage 85 (2014) 711–720.